The Astrophysical Journal, 573:418–424, 2002 July 1

ON THE GENERATION OF FLUX-TUBE WAVES IN STELLAR CONVECTION ZONES. IV. LONGITUDINAL WAVE ENERGY SPECTRA AND FLUXES FOR STARS WITH NONSOLAR METALLICITIES

Z. E. Musielak
Department of Physics, University of Texas, Arlington, TX 76019; zmusielak@uta.edu

R. Rosner
Department of Astronomy and Astrophysics, and Enrico Fermi Institute, University of Chicago, Chicago, IL 60637; rrosner@oddjob.uchicago.edu

and

P. Ulmschneider
Institut für Theoretische Astrophysik, Universität Heidelberg, Tiergartenstrasse 15, D-69121 Heidelberg, Germany; ulm@ita.uni-heidelberg.de
Received 2001 November 26; accepted 2002 March 10

ABSTRACT

In the previous papers of this series, we developed an analytical method describing the generation of longitudinal tube waves in stellar convection zones and used it to compute the wave energy spectra and fluxes for late-type stars with the solar metal abundance (Population I). We now extend these calculations to Population II stars with effective temperatures ranging from $T_{\rm eff} = 2500$ to 10,000 K, gravities $\log g = 3$–5, and with three different metal abundances: 1/10, 1/100, and 1/1000 of solar metallicity. The obtained results are valid for a single magnetic flux, and they show that the effects of metallicity are important only for cool stars with $T_{\rm eff} < 6000$ K and that the amount of the generated wave energy decreases roughly by an order of magnitude for every decrease of the metallicity by an order of magnitude. The maximum wave energy flux generated in Population II stars is 7×10^8 ergs cm^{-2} s^{-1}, and it is practically the same for stars of different gravities and metallicities. The computed spectra and fluxes can be used to construct theoretical models of magnetic regions in chromospheres of Population II stars.

Subject headings: convection — MHD — stars: interiors — stars: late-type — turbulence — waves

1. INTRODUCTION

The main aim of this series of papers (Musielak et al. 1989, 1995, 2000) is to incorporate the highly intermittent spatial magnetic (flux-tube) structures into the theory of wave generation and compute the wave energy fluxes and spectra carried by longitudinal tube waves in atmospheres of late-type dwarfs and giants. In our approach, a thin and vertically oriented magnetic flux tube embedded in a nonmagnetized stellar convection zone is considered, and the interaction of this tube with the external turbulent convection is investigated. As a result of this interaction, the kinetic energy of the convective fluid motions buffeting the tube is converted into longitudinal tube waves, which are essentially slow MHD (or acoustic) waves guided by the tube magnetic field lines. The generated waves propagate along the tube and carry the energy from stellar convection zones to the overlying atmosphere. This energy transfer can be used to explain the enhanced heating observed in magnetized regions of stellar atmospheres (e.g., Linsky 1991) and to construct theoretical models of stellar chromospheres (e.g., Cuntz et al. 1999; Fawzy 2001; Ulmschneider et al. 2001a).

In the first paper of this series (Musielak, Rosner, & Ulmschneider 1989), we developed a general analytical treatment of the interaction between a single magnetic flux tube and the external turbulent motions and derived the basic formulae for the efficiency of generation of linear longitudinal tube waves by a simplified model of turbulent convection. The model was not very accurate when applied to the Sun and other late-type stars; thus, in the next paper (Musielak et al. 1995, hereafter Paper I), we incorporated a more realistic description of the turbulent convection based on the results given by Musielak et al. (1994). The derived formulae were then used to compute the wave energy spectra and fluxes for late-type stars with the solar metal abundance (Musielak, Rosner, & Ulmschneider 2000, hereafter Paper II). We now extend our computation of the generation of longitudinal tube wave energy spectra and fluxes to stars of different metallicity, which refers here to all chemical elements except hydrogen and helium. Similar calculations of the generation of acoustic waves in convection zones of Population I and II stars were performed by Ulmschneider et al. (1996) and (1999), respectively. Population I stars, like the Sun, have a high metal abundance, while Population II stars have 1/10 to 1/100 or sometimes even 1/1000 of the solar metal abundance. We consider late-type stars of Population II with three different metal abundances and use opacity tables calculated with the ATLAS program by Kurucz (1992, 1996). For comparison, we also compute longitudinal wave energy spectra and fluxes by using Kurucz opacity tables for the solar metal abundance and opacity tables originally described by Bohn (1984), which we used in Papers I and II.

The wave energy spectra and fluxes presented in this paper are computed for stars with effective temperatures ranging from $T_{\rm eff} = 2500$ to 10,000 K and gravities in the range of $\log g = 3$–5. Obviously, the effects of metallicity are expected to be different in stars of various spectral types. For hot stars, in which the onset of convection takes place in the region of hydrogen ionization, the opacity is dominated by hydrogen, and the effects of different metal abundances are expected to be small. However, the metal content greatly affects opacity in cool stars; namely, lowering the metallicity decreases the opacity. The latter has an important effect on the upper boundary of the stellar convection

zone, which is "moved" to deeper layers of these stars, where the gas density is much higher. As a result, the efficiency of stellar convection in cool stars of Population II is lower than that for Population I stars of the same spectral types (e.g., Ulmschneider et al. 1999). Note that the upper boundary of the stellar convection zone in hot stars remains unchanged because hydrogen is primarily responsible for the stellar opacity. These effects are clearly shown by the results presented in this paper, which is organized as follows. A brief description of the computational method is given in § 2; the opacity tables used in this paper are described in § 3; the computed stellar wave energy spectra and are presented and discussed in § 4; and final conclusions are given in § 5.

2. METHOD OF COMPUTATION

The analytical treatment of the generation of longitudinal tube waves in stellar convection zones is described in Paper I. The basic formulae are given in Paper II (see eqs. [5]–[9]) and will not be repeated here. These formulae are valid for a single, thin, and vertically oriented magnetic flux tube that is embedded in an atmosphere of a star of given $T_{\rm eff}$ and $\log g$. We assume that the tube diameter at the stellar surface is roughly equal to the local scale height, which means that the tube can be considered as thin and that there are no longitudinal flows inside the tube. To compute longitudinal tube wave energy spectra and fluxes, we must know the model of the flux tube. The most important parameter that uniquely determines the model is the field strength inside the magnetic flux tube. Currently, this field cannot be determined by stellar observations (Saar 1996; Rüedi et al. 1997); therefore, we guide ourselves by solar observations which show that the typical field strength in solar magnetic flux tubes at the solar surface is $B_0 = 1500$ G (e.g., Solanki 1993); this corresponds to approximately $B_0 = 0.85\ B_{\rm eq}$, where $B_{\rm eq} = (8\pi p_e)^{1/2}$ is the equipartition field strength, and p_e is the external gas pressure at the solar surface. In Paper II, we considered three different values of magnetic field strength; namely, $B_0/B_{\rm eq} = 0.75$, 0.85, and 0.95 for Population I stars. In the present paper, we take the same values for Population II stars. In all calculations, the field strength B_0 is specified at the atmospheric optical depth $\tau_{5000} = 1$.

The structure of the nonmagnetized medium that surrounds the tube is calculated by using a stellar envelope computer code described by Bohn (1984) and later modified by Theurer (1993) and Ulmschneider et al. (1996). The input parameters to the code are $T_{\rm eff}$, g, and the mixing-length parameter $\alpha = l_{\rm mix}/H$, where $l_{\rm mix}$ is the mixing length and H is the pressure scale height. According to Paper II, we assume that $\alpha = 2$ in most of our calculations. For comparison, we also compute wave energy fluxes with $\alpha = 1$ and 1.5 for stars with $\log g = 4$. By specifying α, the code gives a stellar convection zone model, which is then employed as a model for the external medium. The model and the horizontal pressure balance (determined for a given strength of the tube magnetic field) are then used to compute the structure of the background medium inside the tube at different atmospheric heights. To calculate the external and internal models, we must have opacity tables valid for the reduced metallicity observed in Population II stars. In the following, we describe our choice of the opacity tables for these stars.

3. OPACITY TABLES

The results presented in Paper II for Population I stars were obtained by using opacity tables compiled by Bohn (1984) and Theurer (1993) from various opacity tables given by Alexander (1975, 1989), Cox & Tabor (1976), Yorke (1979, 1980), Meyer-Hofmeister (1982), and Weiss (1990). Here we refer to these tables as the *Bohn opacity*, and they are valid for the solar chemical abundance, i.e., abundance by mass of hydrogen $X_m = 0.70$, helium $Y_m = 0.28$, and of metals $Z_m = 2 \times 10^{-2}$. To account for the reduced metallicity observed in Population II stars, we use the opacity tables calculated with the ATLAS program of Kurucz (1992, 1996). We refer to these tables as the *Kurucz opacity*, and they are available for the following solar and nonsolar metal abundances: $Z_m = 2 \times 10^{-2} \mathrel{\hat{=}} [0]$, $Z_m = 2 \times 10^{-3} \mathrel{\hat{=}} [-1]$, $Z_m = 2 \times 10^{-4} \mathrel{\hat{=}} [-2]$, and $Z_m = 2 \times 10^{-5} \mathrel{\hat{=}} [-3]$, where the logarithm of the reduction factor is given in square brackets. (Bracket notation for metallicity will be used in the remaining part of this paper.)

Thus, the wave energy spectra and fluxes presented in this paper for Population II stars are obtained with the Kurucz opacity [−1], [−2], and [−3]. For comparison, we also compute the spectra and fluxes by using the Kurucz opacity [0] and the Bohn opacity. The range of validity of these opacity tables is shown and discussed by Ulmschneider et al. (1999; see their Fig. 1). The limited range of these opacity tables imposes some restrictions on the convection zone models that can be computed. For example, high temperatures and densities present in deep layers of stellar convection zones typically exceed the range of these parameters in the opacity tables.

Fortunately, the most efficient generation of longitudinal tube waves takes place mainly in the subphotospheric layers, and the contribution from the deep layers is always negligible. Hence, the deepest layer in our convection zone models is calculated with the last entry of the opacity table before the range of this table is exceeded. Another problem is the low temperature and density limit of the opacity tables and uncertainties in the values of opacities for low $T_{\rm eff}$. Because of these problems, we consider only stars with $T_{\rm eff} \geq 2500$ K and terminate our computations of stellar convection zone models if temperatures and densities in the outermost layers of these models fall outside the lower boundary of the opacity table.

4. RESULTS AND DISCUSSION

As shown in Papers I and II, our analytical approach describes the generation of propagating longitudinal tube waves, which implies that only wave frequencies higher than the cutoff frequency for longitudinal tube waves are allowed. In our computation, we assume that the wave frequency domain extends from $\omega = 1.002\ \Omega_L$ to $57\ \Omega_L$, where Ω_L is the cutoff frequency first introduced by Defouw (1976). The wave energy fluxes carried by longitudinal tube waves in stellar atmospheres are calculated by performing the Laguerre integration over the wave frequency ω by using 32 points within the frequency domain. In addition, the shape of the turbulent energy spectrum and the so-called frequency factor (see Papers I and II) are assumed to be the same in all considered stars. The presented results are obtained for a single magnetic flux tube embedded in the convection zone of a late-type star of different $T_{\rm eff}$ and $\log g$.

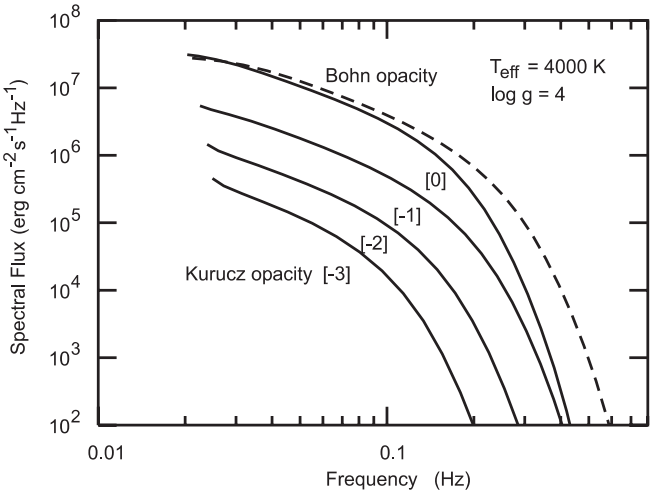

FIG. 1.—Longitudinal wave energy spectra plotted for stars with $T_{\rm eff} = 4000$ K, $\log g = 4$, and different metallicities. The results were obtained for a mixing-length parameter $\alpha = 2$ and a magnetic field strength $B_0 = 0.85\ B_{\rm eq}$ at $\tau_{5000} = 1$.

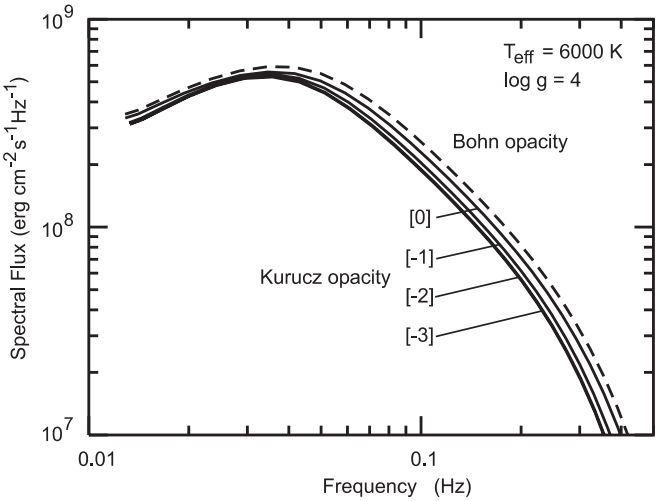

FIG. 2.—Same as Fig. 1, but for $T_{\rm eff} = 6000$ K

This means that the filling factor, representing the number of magnetic flux tubes per unit area of the stellar surface, will not be discussed in this paper.

4.1. *Wave Energy Spectra*

The wave energy spectra calculated for stars with the same effective temperature, $T_{\rm eff} = 4000$ K, and gravity $\log g = 4$, but different metallicities are presented in Figure 1: note that the calculations were performed by taking $\alpha = 2$ and $B_0/B_{\rm eq} = 0.85$. It is seen that the shapes of these spectra computed for Population II stars with metallicities [−1], [−2], and [−3] and for Population I stars with the solar metallicity (Bohn opacity) are very similar. However, the shape of the spectrum obtained for Population I stars with the Kurucz [0] opacity differs significantly from the other spectra for high frequencies. There is also noticeable decrease in the generated wave energy flux with decreasing metallicity; this effect is most prominent at high frequency and can be explained as follows. Stellar convection stops when the rising convective gas bubbles reach a height (near the stellar surface) at which the opacity is so low that the excess thermal energy of the bubbles is radiated directly into space. By lowering the opacity, this height is reached at deeper layers, where the density ρ is higher, and because the total stellar radiative flux $\sigma T_{\rm eff}^4 \approx \rho v_{\rm conv}^3$, the convective velocity $v_{\rm conv}$ becomes correspondingly smaller. As a result, the efficiency of generation of longitudinal tube waves also decreases.

It is now interesting to compare the above results to those given in Figure 2, which shows the wave energy spectra computed for stars with $T_{\rm eff} = 6000$ K, $\log g = 4$, $\alpha = 2$, and $B_0/B_{\rm eq} = 0.85$. Clearly, the presented spectra are almost identical and show very little dependence on metallicity. This can be explained by the fact that the opacity in hot stars is mainly due to hydrogen, which is not affected by changes in metallicity. However, in cool stars (see Fig. 1) the opacity is mainly due to metals—thus, its strong dependence on the metal abundance. The comparison also shows that the amount of wave energy carried by longitudinal tube waves of the same frequency in cool stars strongly decreases with decreasing metallicity, that the generated wave energy flux for a given frequency is always much higher for hot stars than for cool stars, and that the computed wave energy spectra are relatively flat at high $T_{\rm eff}$, yet become much steeper when $T_{\rm eff}$ is decreased. Finally, it must be noted that for both hot and cool stars, the longitudinal wave energy spectra extend more than 1 order of magnitude above the cutoff frequency.

4.2. *Dependence on Physical Parameters*

The mixing-length parameter α and the strength of the magnetic field, $B_0/B_{\rm eq}$, are two basic physical parameters in our calculations. To study their effects on the computed stellar wave energy fluxes, we consider Population II stars with $\log g = 4$, metallicity [−3], and different effective temperatures, $T_{\rm eff}$, and take $\alpha = 1$, 1.5, and 2 for fixed $B_0 = 0.85\ B_{\rm eq}$, and alternatively $B_0/B_{\rm eq} = 0.75$, 0.85, and 0.95 for fixed $\alpha = 2$. The obtained results are presented in Figures 3 and 4.

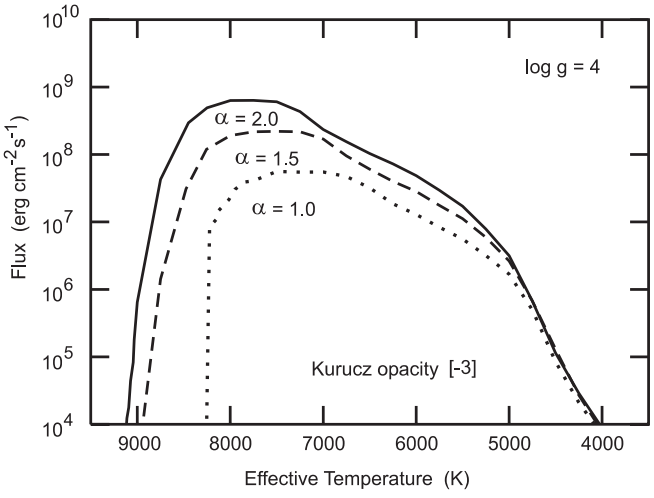

FIG. 3.—Longitudinal wave energy fluxes computed for stars of different spectral types are plotted for three different values of the mixing-length parameter $\alpha = 1$, 1.5, and 2. Fluxes were obtained for stars with $\log g = 4$, metallicity [−3], and a magnetic field strength $B_0 = 0.85\ B_{\rm eq}$ at $\tau_{5000} = 1$.

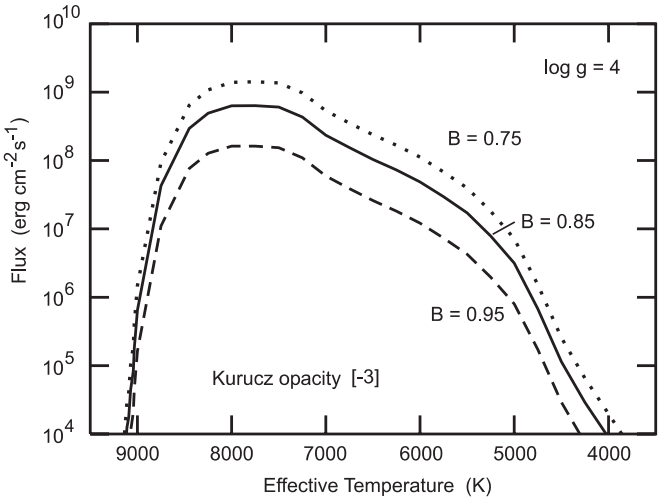

FIG. 4.—Longitudinal wave energy fluxes computed for stars of different spectral types are plotted for three different values of the tube magnetic field: $B_o/B_{eq} = 0.75$, 0.85, and 0.95 specified at $\tau_{5000} = 1$. Fluxes were obtained for stars with $\log g = 4$, metallicity [−3], and a mixing-length parameter $\alpha = 2$.

According to Figure 3, the α-dependence is relatively weak for cool stars; however, significant differences in the generated wave energy fluxes are seen for hot stars. These differences can be explained by the higher efficiency of stellar convection in hot stars and its high sensitivity to the value of α. The dependence of these fluxes on α increases with increasing T_{eff} and is especially prominent for stars with $T_{eff} > 7000$ K. Now the results of Figure 4 show that the magnetic field dependence is strong for all considered stars except the hottest ones, with $T_{eff} > 8500$ K. It is also seen that the wave energy fluxes increase with decreasing magnetic field strength. This dependence can be explained by decreasing stiffness of the tube for weaker tube magnetic fields (see Paper I). Note that the dependence of the generated wave energy fluxes on both α and B_0 found here for Population II stars is very similar to that obtained in Paper II for Population I stars.

The dependence of the wave energy fluxes on the mixing-length parameter, α, for a given star with $T_{eff} = 6000$ K, $\log g = 4$, and metallicity [−3] is given in Table 1. Based on these results, we find that the dependence of F_L on α can be approximated by

$$F_L \approx 1.3 \times 10^7 \ \alpha^{1.9} \text{ ergs cm}^{-2} \text{ s}^{-1} . \quad (1)$$

The derived α-dependence is similar to that found for the longitudinal wave generation rate in the Sun (Paper I) and other Population I stars (Paper II).

Table 1 also shows that the total wave energy flux (F_L) decreases with increasing magnetic field strength, B_0/B_{eq}. This dependence can approximately be fitted by the expression

$$F_L \approx 8.0 \times 10^6 \left(\frac{B_0}{B_{eq}}\right)^{-9.2} \text{ ergs cm}^{-2} \text{ s}^{-1} . \quad (2)$$

Again, this dependence is very similar to that found for the Sun in Paper I and for Population I stars in Paper II. (See also Ulmschneider, Musielak, & Fawzy 2001b.) This simply means that the dependence of the longitudinal wave generation on the tube magnetic field does not change when stellar metallicity is decreased.

Based on these results, we conclude that the effects caused by the mixing-length parameter, α, and the tube magnetic field, B_0/B_{eq}, on the rate of the generation of longitudinal tube waves are independent of stellar metallicity.

TABLE 1

LONGITUDINAL WAVE ENERGY FLUXES FOR DIFFERENT VALUES OF THE MIXING-LENGTH PARAMETER α AND TUBE MAGNETIC FIELD B_0/B_{EQ} (IN ERGS CM^{-2} S^{-1})

α	B_0/B_{eq}	F_T
1.0.....	0.85	1.3×10^7
1.5.....	0.85	2.8×10^7
2.0.....	0.85	4.9×10^7
2.0.....	0.75	1.1×10^8
2.0.....	0.95	1.2×10^7

NOTE.—Fluxes were computed for a star with $T_{eff} = 6000$ K, $\log g = 4$, and metallicity [−3].

4.3. *Stellar Wave Energy Fluxes*

The longitudinal wave energy fluxes computed for stars with different effective temperatures and metallicity are shown in Figures 5, 6, and 7, which are arranged in order of decreasing gravity from $\log g = 5$–3. The presented results clearly show that the effects of metallicity are important only in cool stars with $\log g = 5$ and $T_{eff} < 6000$ K, with $\log g = 4$ and $T_{eff} < 5500$ K, and with $\log g = 3$ and $T_{eff} < 5000$ K. It is seen that the wave energy fluxes for cool stars of Population II decrease roughly by an order of magnitude for every decrease of the metallicity by an order of magnitude and that this effect is independent of stellar gravity. Note also that there are discrepancies between the wave energy fluxes calculated by using the Kurucz opacity tables

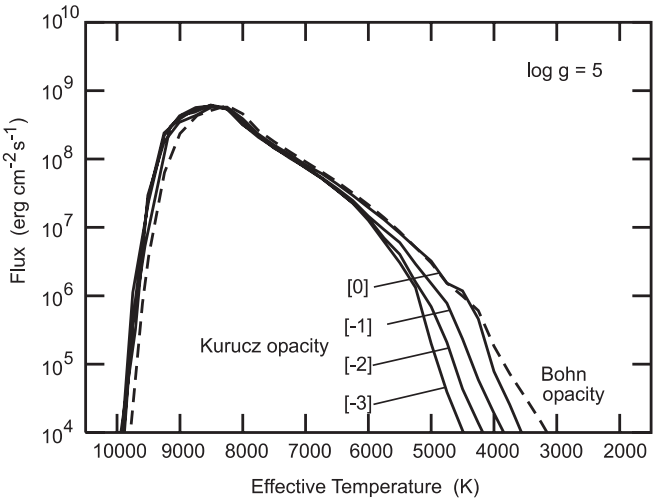

FIG. 5.—Longitudinal wave energy fluxes computed for stars of different spectral types and different metallicities. Fluxes were obtained for stars with $\log g = 5$, the mixing-length parameter $\alpha = 2$, and for the tube magnetic field $B_0 = 0.85\ B_{eq}$ at $\tau_{5000} = 1$.

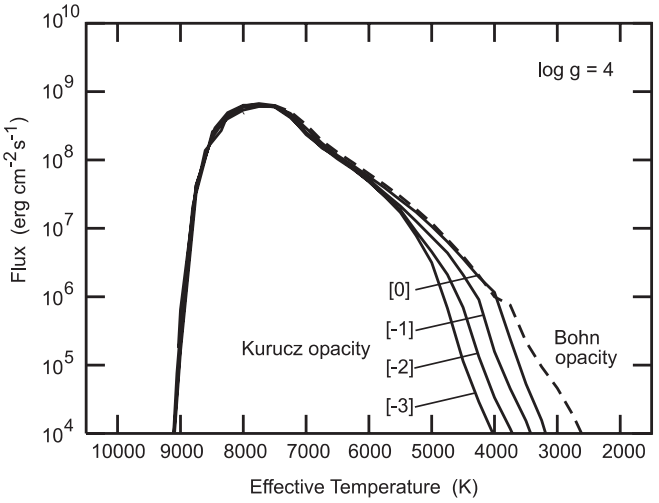

FIG. 6.—Same as Fig. 5, but for $\log g = 4$

with metallicity [0] and the Bohn opacity tables. These discrepancies are especially prominent for cool stars with $T_{\rm eff} < 4000$ K, and they increase with decreasing gravity. As already explained by Ulmschneider et al. (1999), the most likely reason for these discrepancies is the limited range of the used opacity tables.

For hot stars with $\log g = 5$ and 4, the wave energy fluxes are practically identical (see Figs. 5 and 6; Table 2). The stars with the highest effective temperatures, where the wave fluxes rise very rapidly, are strongly affected by the onset of convection. This is because of the onset of the hydrogen ionization, which influences the adiabatic gradient and occurs at progressively lower $T_{\rm eff}$ and lower gravity. In these stars, the convection zones are very narrow and the computed values of convective velocities become sensitive to the numerical integration steps. As a result, the wave energy fluxes strongly vary with small changes in $T_{\rm eff}$, and the effect leads to differences in the computed fluxes for hot stars with $\log g = 3$ (Fig. 7). It must also be mentioned that the maximum convective velocities in some of these stars approach the sound speed, which implies that the obtained fluxes are unrealistic (Paper II).

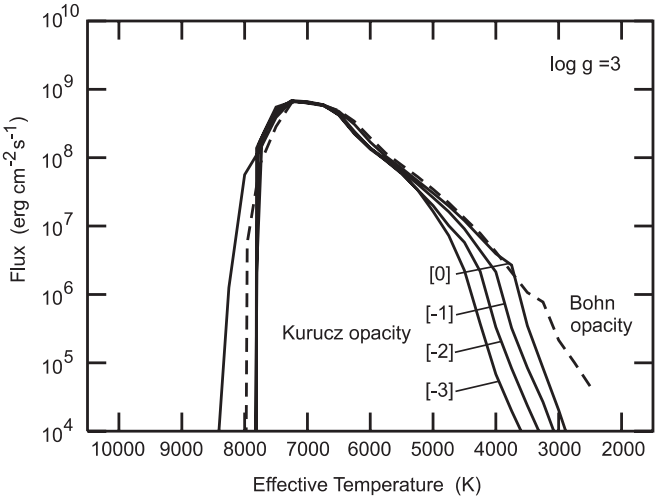

FIG. 7.—Same as Fig. 5, but for $\log g = 3$

TABLE 2

WAVE ENERGY FLUXES FOR UPWARD PROPAGATING LONGITUDINAL TUBE WAVES IN STARS WITH DIFFERENT EFFECTIVE TEMPERATURES, GRAVITY, AND METALLICITY (IN ERGS CM^{-2} S^{-1})

$T_{\rm eff}$	$\log g = 3$	$\log g = 4$	$\log g = 5$
Metallicity [0]			
3000	2.0×10^4	2.7×10^3	3.0×10^2
5000	3.0×10^7	1.1×10^7	3.2×10^6
7000	6.4×10^8	2.9×10^8	8.3×10^7
9000	...	1.6×10^5	3.4×10^8
Metallicity [−1]			
3000	6.5×10^3	7.9×10^2	7.8×10^1
5000	2.6×10^7	7.5×10^6	1.5×10^6
7000	6.3×10^8	2.5×10^8	7.7×10^7
9000	...	2.8×10^5	4.4×10^8
Metallicity [−2]			
3000	1.8×10^3	1.8×10^2	8.7×10^0
5000	2.0×10^7	4.6×10^6	6.9×10^5
7000	6.4×10^8	2.5×10^8	7.4×10^7
9000	...	2.0×10^5	3.8×10^8
Metallicity [−3]			
3000	4.7×10^2	3.6×10^1	2.4×10^{-1}
5000	1.6×10^7	3.2×10^5	2.0×10^5
7000	6.6×10^8	2.3×10^8	7.5×10^7
9000	...	6.5×10^5	4.3×10^8

NOTE.—Fluxes were computed by using the mixing-length parameter $\alpha = 2$ and the tube magnetic field $B_0 = 0.85\ B_{\rm eq}$ at $\tau_{5000} = 1$.

The convective velocities in cooler stars are lower than in hot stars and, therefore, the calculated longitudinal wave energy fluxes are also lower. In addition, these fluxes strongly depend on metallicity, which can be explained by the fact that for cool stars, the main contribution to the opacity is from metals, while for hot stars, the opacity is mainly determined by hydrogen (§ 4.1). This means that the metallicity does not affect hot stars, but it is important for cool stars (Figs. 5, 6, and 7; Table 2).

The influence of gravity on the wave energy fluxes computed for stars with metallicities ranging from [−1] and [−3] are shown in Figures 8 and 9, respectively. These results are obtained for $\alpha = 2$ and $B_0 = 0.85\ B_{\rm eq}$. Both figures show that the efficient excitation of longitudinal tube waves occurs at higher $T_{\rm eff}$ for hot dwarfs with $\log g = 5$ than for giants with $\log g = 3$. An additional problem is that for some giants considered here, the ratio of the maximum convective velocity to the local sound speed (the so-called convective Mach number) can exceed 1 (see Ulmschneider et al. 2001b, and their Fig. 1). According to the results presented in Paper II, the wave energy fluxes computed for stars with $T_{\rm eff} > 8000$ K and $\log g = 4$ and with $T_{\rm eff} > 7000$ K and $\log g = 3$ might not be realistic. The same restrictions apply to the Population II stars considered in this paper.

The results presented in Figures 8 and 9 also show that stars with lower gravities but similar effective temperature

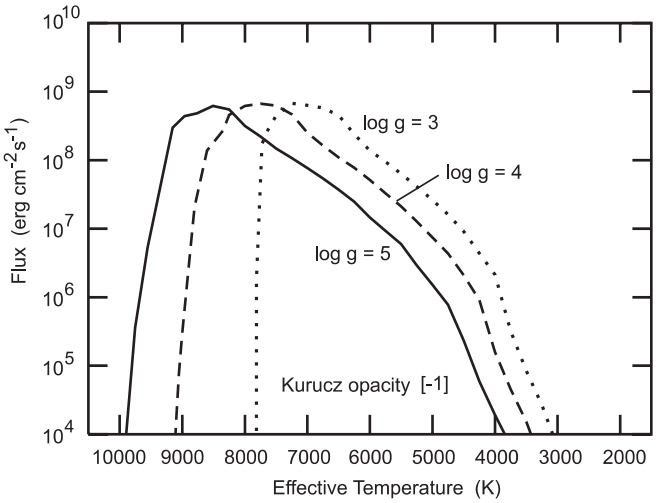

FIG. 8.—Longitudinal wave energy fluxes computed for stars of different spectral types and different gravities. Fluxes were obtained for stars with the metallicity [−1], the mixing-length parameter $\alpha = 2$, and for the tube magnetic field $B_0 = 0.85\ B_{eq}$ at $\tau_{5000} = 1$.

produce higher longitudinal wave energy fluxes. These fluxes rapidly increase with increasing T_{eff} until they reach their maxima at about 7×10^8 ergs cm^{-2} s^{-1}. The maxima are practically the same for stars of different gravities and metallicities, and they occur for A or early F stars just before convection ceases to exist in these stars at higher effective temperatures. By comparing the fluxes obtained with metallicity [−1] and [−3], one sees that the range of T_{eff} for which the wave energy flux is higher than 1.0×10^4 ergs cm^{-2} s^{-1} gets smaller with decreasing metallicity. This effect is most prominent for the coolest stars considered in this paper (see also Table 2).

We now compare our results to those obtained previously for the generation of acoustic (Ulmschneider et al. 1999) and transverse tube (Musielak & Ulmschneider 2002) waves in Population II stars. According to these authors, late-type stars can be divided into three groups labeled I, II, and III, which represent regions in the H-R diagram with different dependences of the acoustic and transverse tube wave generation on the stellar metal abundance. For hot stars of group I, there is no dependence of the generated wave fluxes on metallicity. For cool stars of group III, the wave generation strongly depends on the metallicity, and the generated wave energy fluxes are lowered roughly by an order of magnitude for every decrease of the metallicity by an order of magnitude. Finally, stars of group II represent the transition between the other two groups, and the generated fluxes become a sensitive function of the effective temperature. Since the results presented in this paper for longitudinal tube waves are in full agreement with those previously obtained for acoustic and transverse tube waves, we conclude that the effects of metallicity on the wave generation process are very similar for nonmagnetic and magnetic waves.

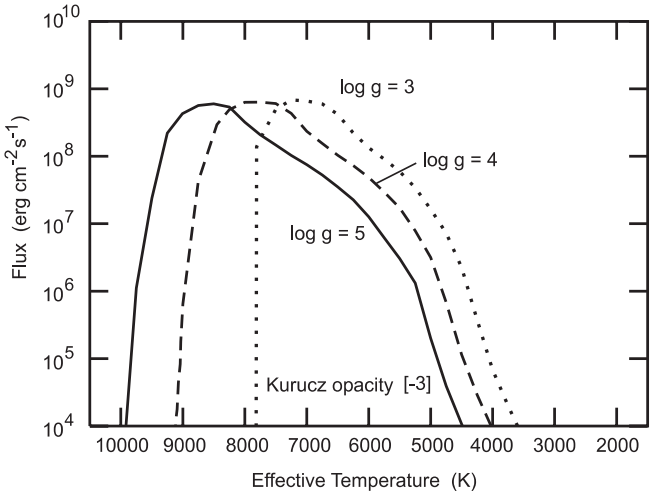

FIG. 9.—Same as Fig. 8, but for the metallicity [−3]

5. CONCLUSIONS

From our studies of the generation of longitudinal tube waves propagating along a single magnetic flux tube embedded in atmospheres of late-type stars with different metallicities, the following conclusions can be drawn.

1. The shapes of the computed wave energy spectra are similar for stars of the same effective temperature and gravity but different metallicity.
2. The effects caused by the mixing-length parameter and the tube magnetic field on the rate of generation of longitudinal tube wave are independent of stellar metallicity.
3. The effects of metallicity are important for stars with $\log g = 5$ and $T_{eff} < 6000$ K, $\log g = 4$ and $T_{eff} < 5500$ K, and $\log g = 3$ and $T_{eff} < 5000$ K, and the amount of the generated wave energy decreases roughly by an order of magnitude for every decrease of the metallicity by an order of magnitude.
4. For hot stars with $T_{eff} > 6000$ K, the generated wave energy fluxes are practically independent of metallicity. However, for stars with $\log g = 5$ and $T_{eff} > 9500$ K, $\log g = 4$ and $T_{eff} > 8500$ K, and $\log g = 3$ and $T_{eff} > 7500$ K, the wave generation becomes very sensitive to small changes in T_{eff}. As the convective velocities approach the sound speed for these stars, the longitudinal wave fluxes are not very reliable.
5. The maximum wave energy flux generated in Population II stars is about 7×10^8 ergs cm^{-2} s^{-1}, and it is practically the same for stars of different gravities and metallicities.
6. Comparing our results to those obtained by Ulmschneider et al. (1999) for acoustic waves and Musielak & Ulmschneider (2002) for transverse tube waves shows that the effects of metallicity on the wave generation process are very similar for nonmagnetic and magnetic waves.
7. Finally, it must be noted that the computed wave energy fluxes may be insufficient to account for the full range of chromospheric activity observed in late-type stars. (See Ulmschneider et al. 2001a.)

This work was supported by NSF under grant ATM-0087184 (Z. E. M. and P. U.), by the DFG grant Ul57/25-3, and by NATO under grant CRG-910058 (P. U. and Z. E. M.). Z. E. M. also acknowledges the support of this work by the Alexander von Humboldt Foundation.

REFERENCES

Alexander, D. R. 1975, ApJS, 29, 363
———. 1989, ApJ, 345, 1014
Bohn, H. U. 1984, A&A, 136, 338
Cox, A. N., & Tabor, J. E. 1976, ApJS, 31, 271
Cuntz, M., Rammacher, W., Ulmschneider, P., Musielak, Z. E., & Saar, S. H. 1999, ApJ, 522, 1053
Defouw, R. J. 1976, ApJ, 209, 266
Fawzy, D. E. 2001, Ph.D. thesis, Univ. Heidelberg, Germany
Kurucz, R. L. 1992, in IAU Symp. 149, The Stellar Population of Galaxies, ed. B. Barbuy & A. Renzini (Dordrecht: Kluwer)
———. 1996, in ASP Conf. Ser. 108, Workshop on Model Atmospheres and Spectrum Synthesis, ed. S. J. Adelman, F. Kupka, & W. Weiss (San Francisco: ASP)
Linsky, J. L. 1991, in Heidelberg Conf., Mechanisms of Chromospheric and Coronal Heating, ed. P. Ulmschneider, E. Priest, & R. Rosner (Berlin: Springer), 166
Meyer-Hofmeister E. 1982, in Stellar Structure and Evolution, ed. K. Schaifers & H. H. Voigt (Berlin: Springer)
Musielak, Z. E., Rosner, R., Gail, H.-P., & Ulmschneider, P. 1995, ApJ, 448, 865 (Paper I)
Musielak, Z. E., Rosner, R., Stein, R. F., & Ulmschneider, P. 1994, ApJ, 423, 474
Musielak, Z. E., Rosner, R., & Ulmschneider, P. 1989, ApJ, 337, 470
———. 2000, ApJ, 541, 410 (Paper II)
Musielak Z. E., & Ulmschneider P. 2002, A&A, in press
Rüedi, I., Solanki, S. K., Mathys, G., & Saar, S. H. 1997, A&A, 318, 429
Saar, S. H. 1996, in IAU Symp. 176, Stellar Surface Structure, ed. K. Strassmeier & J. L. Linsky (Dordrecht: Kluwer), 237
Solanki, S. K. 1993, Space Sci. Rev., 63, 1
Theurer, J. 1993, Diploma thesis, Univ. Heidelberg, Germany
Ulmschneider, P., Fawzy, D. E., Musielak, Z. E., & Stępień, K. 2001a, ApJ, 559, L167
Ulmschneider, P., Musielak, Z. E., & Fawzy, D. E. 2001b, A&A, 374, 662
Ulmschneider, P., Theurer, J., & Musielak, Z. E. 1996, A&A, 315, 212
Ulmschneider, P., Theurer, J., Musielak, Z. E., & Kurucz, R. 1999, A&A, 347, 243
Weiss, A. 1990, At. Data Nucl. Data Tables (2), 45, 209
Yorke, H. W. 1979, A&A, 80, 308
———. 1980, A&A, 85, 215